MNE 19 (2023) 100185

Contents lists available at ScienceDirect

Micro and Nano Engineering

journal homepage: www.sciencedirect.com/journal/micro-and-nano-engineering

# Biodegradable materials as sensitive coatings for humidity sensing in S-band microwave frequencies

James Bourely [a,*], Leticia De Sousa [a], Nicolas Fumeaux [a], Oleksandr Vorobyov [b], Christian Beyer [b], Danick Briand [a,*]

[a] École Polytechnique Fédérale de Lausanne (EPFL), Soft Transducers Laboratory (LMTS), Neuchâtel 2000, Switzerland
[b] Centre Suisse d'électronique et de Microtechnique (CSEM), Neuchâtel 2002, Switzerland

ARTICLE INFO

*Keywords:*
Biodegradable humidity sensor
S-band microstrip resonator
Psyllium
Konjac glucomannan
Egg-albumin
Beeswax

ABSTRACT

Worldwide, electronic waste represents the fastest-growing stream of waste. With an increasing number of connected devices, passive and eco-friendly environmental sensing solutions need to be developed. Wireless passive devices for RFID and sensing exist, however, most of them rely on non-biodegradable materials. Willing to produce entirely green radio-frequency (RF) resonators on a paper substrate, we identify potential biodegradable materials to be used as encapsulation and humidity sensing layers. Resonator encapsulation is mandatory to prevent humidity interaction with the transducer while a sensing layer above the resonator enables a good response to humidity. In this work, the radio-frequency behavior of these materials was characterized when implemented on a 3.3 GHz resonating microstrip structure made of copper on FR4 substrate. The response in resonance frequency while varying the relative humidity (RH) from 20% to 80% was monitored. Beeswax-coated resonators exhibited no change in resonance frequency when exposed to humidity and therefore provided excellent encapsulation properties. 10 μm-thick layers of psyllium, konjac and egg-albumin displayed suitable sensing behavior with suitable frequency shifts above 100 MHz from 20% to 80% RH. Konjac and psyllium showed the best compatibility when coated on the beeswax encapsulant, exhibiting reversibility and low hysteresis when exposed to humidity variations.

## 1. Introduction

According to the 2020 report from the United Nations [1], electronic waste represents the fastest-growing stream of waste. It is reaching 8 kg per person annually. Worldwide, with the rise of the Internet of Things (IoT), the number of connected devices, that are mainly composed of toxic and environmentally harmful elements, is increasing [2,3]. Simultaneously, the number of sensors deployed increases at a high pace, due to the exploiting rise of smart products, facilitating ubiquitous sensing [4]. Notably, most of these systems applied for tracking temperature and humidity in the field of logistics are discarded [5]. Therefore, having biodegradable systems would reduce their environmental impact.

Relative Humidity (RH) sensors implementing eco-friendly materials have been reported using the substrate as moisture responsive material or by adding a specific sensitive coating. Cellulose is a biodegradable, renewable and widely available [6] resource and has been commonly used as humidity sensitive substrates. These paper-based sensing devices have relied on capacitive [7–11] and resistive [12] detections mechanisms where the presence of moisture modifies the dielectric and electrical properties between interdigitated electrodes patterned on the substrate. But, using paper which exhibit a slow diffusion rate can lead to slow response times and hysteresis [7,11,13]. Other recyclable and compostable substrates such as polylactic acid (PLA) [14], chitosan [15], polyethylene terephthalate (PET) or starch [16], have also shown sensitivity to humidity in air. An approach pursued to enhance sensing performances has been to implement an eco-friendly moisture-sensitive coating on the transducer. Humidity sensing characteristics of egg-albumin [11,17], starch and onion membranes [18], salt [19], silk [20] and graphene oxide [21] were analyzed when coated on capacitive platforms made on various types of biodegradable substrates while hydroxyapatites [22] and wheat gluten [23] were tested on FR4. An eco-friendly self-powered humidity sensor has also been demonstrated based on a Cu/NaCl paper/Al primary battery structure [24]. Wireless

* Corresponding authors.
*E-mail addresses:* james.bourely@epfl.ch (J. Bourely), danick.briand@epfl.ch (D. Briand).

https://doi.org/10.1016/j.mne.2023.100185
Received 14 December 2022; Received in revised form 9 March 2023; Accepted 3 April 2023
Available online 5 April 2023

configuration based on recyclable or biodegradable substrates have been reported in the literature for moisture monitoring [25–27]. Despite involving eco-friendly materials, all those humidity sensing platforms still necessitate the use of silicon-based components for signal read-out and data communication [7,9]. To prevent the use of silicon electronics targeting more sustainable sensing systems, researchers have notably adopted a chipless approach.

Monitoring of relative humidity using a wireless and chipless approach based on a resonator is of interest since it does not require the use of any silicon components [28] and can be applied for disposable sensing tags [29]. Those sensing resonators are made of a metallic resonating transducer, forming an RLC circuit, using the substrate itself or a specific coating as humidity sensitive layer. Their resonance frequency depends on the capacitance of the structure, and this capacitance is proportional to the permittivity of the sensing material [30]. These types of devices function at high frequencies (3–30 MHz) or ultra-high frequencies (300 MHz - 3 GHz), which gives them an operational range of a few centimeters up to meters [28,31,32]. Typically relying on standard FR4 printed circuits, with copper for high signal transmission, resonance and quality factor [33,34], researchers have started adopting the chipless configuration and combining it with biodegradable sensitive materials to monitor humidity. Wireless and chipless humidity sensors have been developed using paper as a substrate and an RLC resonating structure made of copper [35], silver [36,37] or aluminium [38]. Polyvinyl-alcohol-coated [33,39,40] and a keratin-coated [41] resonators demonstrated humidity sensitivity in a chipless and wireless setup. However, despite implementing green materials in their configuration, the transducing layers are not biodegradable [42]. To our knowledge, only a zinc and polylactic acid resonator to measure volumetric water concentration in soil has been made fully biodegradable [43].

Envisioning a fully biodegradable chipless resonator functioning in the S-band (2 GHz – 4 GHz) for monitoring humidity in air would require to implement paper or biopolymer substrates coated with degradable functional materials, metallic (i.e. Zn or Mg) and sensing layers. To prevent water sorption that could potentially affect the RF transducer's performances and lead as well to its degradation, its encapsulation would need to be considered as well.

In this study, we have focused on evaluating for the first time various biodegradable dielectric materials in the S-band for future implementation in eco-friendly wireless and chipless humidity sensors. Two types of dielectric materials, encapsulant to protect the transducer against moisture and humidity-sensitive materials, are considered. Those biodegradable materials are coated on a microstrip resonator to assess their humidity response in S-band microwave frequencies, from 2.5 GHz to 3.5 GHz, characterizing their shift in resonance frequency when exposed to variations in humidity. Using simulation, we investigate the optimal coverage area of the microstrip line resonator with the functional materials and the effect of the encapsulation on its resonance frequency. We demonstrate for the first time that super absorbent polymers like konjac and psyllium display good sensitivity to humidity in the S-band (3 GHz) with induced frequency shift of >100 MHz for a change in humidity of 20% to 80% RH. Combining them with a beeswax protective coating provided encapsulation to the underlying substrate and microstrip resonator while maintaining suitable sensing capabilities.

## 2. Material and methods

### 2.1. Device

#### 2.1.1. Microstrip line and sensing mechanism

The humidity test platform presented in this work is composed of a microstrip line resonator. The device is made using a 1.55 mm thick FR4 board with a 12 μm thick copper top and ground layer. The 50 Ω pristine copper/FR4 microstrip line is 3.3 mm wide and incorporates a spiral-shaped resonator with a resonance frequency at 3.3 GHz without coating. The dimensions of the microstrip line are summarized in Fig. 1A.

A spiral configuration embedded within the microstrip line was used as it allows to create a resonating structure without increasing the coverage area of the electrically conductive material comprising the microstrip line. The spiral resonator acts as a stopband filter [31,44] that introduces attenuation in the transmitted signal at its resonant frequency.

Microstrip transmission lines can be modeled by an equivalent RLC circuit [45]. A simplified expression of the frequency of resonance is $f_0 = \frac{1}{\sqrt{LC}}$ in which the capacitor C depends on the permittivity ε of the materials composing the resonator [46]. The loss tangent of the structure is defined by $tan\ \delta = \frac{\varepsilon_r}{\varepsilon_{im}}$ where $\varepsilon_r$ and $\varepsilon_{im}$ are the real and imaginary part of the relative permittivity [47]. As the relative humidity increases, so does the adsorption of water molecules. The water sorption with a much higher permittivity of 80 will induce an increase in the real permittivity of the humidity sensitive materials composing the resonator. Both the equivalent capacitor of the system and the loss tangent will rise. This will lead to a drop in the resonance frequency which is depending on the capacitance value of the system as seen in the schematic of Fig. 1B. With an increase in the dielectric loss, the quality factor of the resonator Q will drop leading to a reduction in the amplitude of the signal. By adding a humidity sensitive coating over the resonator, this phenomenon can be enhanced. Additionally, biodegradable materials tend to be hygroscopic and can exhibit swelling at high humidity. Swelling might modify the geometrical properties of the resonator increasing the dielectric losses [48]. However, we will investigate the overall response to relative humidity changes as analyzing the contribution of humidity on the swelling would require quantifying the change in dimensions of the layers in real-time.

For the RF characterization, the microstrip line is connected to a vector network analyzer (E5071C Agilent) using SMA connectors and the S12 transmission signal is recorded.

#### 2.1.2. Coating materials

Two different types of biodegradable coatings have been investigated: encapsulating and humidity-sensitive layers. The role of the encapsulation layer is to prevent moisture interaction with the transducer, here the copper/FR4 microstrip, which ultimately, in a fully biodegradable configuration, would be replaced by paper and a biodegradable metal.

A proper encapsulation should be hydrophobic in order to prevent water adsorption. The thickness should not be too thick in order to limit RF losses and maintain permittivity shift near the resonator when stacked with a humidity sensitive layer. An encapsulation too thin would not protect the transducing layer and substrate from water permeation. Over a resonator, this encapsulation should prevent any shift in resonant frequency when relative humidity is changing.

The biodegradable materials investigated for encapsulation are POMaC, PGS and Beeswax. These materials have been used in implantable wireless high-frequency applications [49,50] but their moisture protective capabilities were never studied on resonators.

POMaC, a stretchable elastomeric biomaterial, was synthesized following [51] using citric acid, maleic anhydride and 1,8-octanediol. Two POMaC versions were tested, one using UV-curable photo-initiators and one without. The solutions were blade casted onto the resonator and either photocured at room temperature for 1 h or oven cured at 130 °C for 24 h. PGS, a biodegradable elastomer, is synthesized following [52] recipe. This polyester is drop casted onto the resonator and cured at 130 °C for 24 h. The targeted thickness for the PGS and POMaC encapsulants was 100 μm. Beeswax is a natural wax that is used as a waterproofing agent in transient electronics [49]. It was considered due to its hydrophobic properties obtained from the poly- and mono-saturated esters and fatty acids composing their molecular structure.

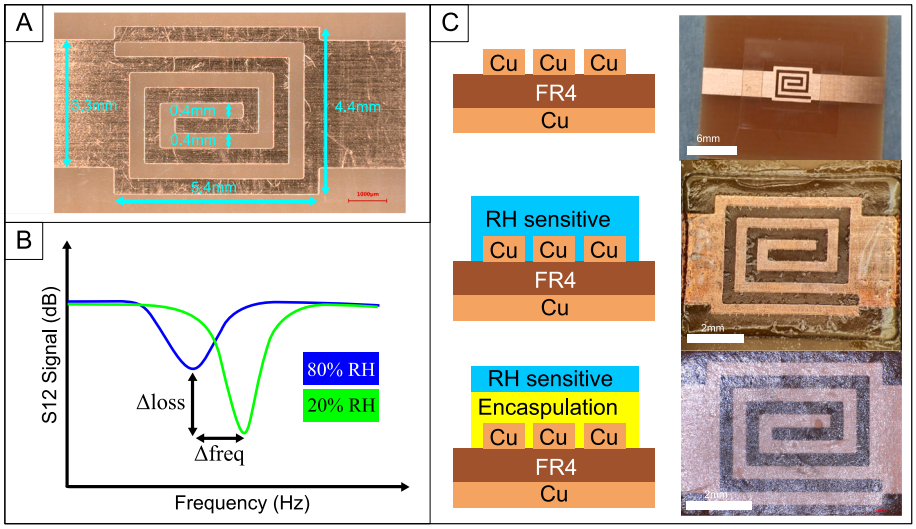


**Fig. 1.** A) Dimensions of the microstrip line platform. B) Theoretical humidity response behavior of a microstrip line resonator C) Schematic cross-sections and top view images of the devices used in this study. Top: pristine FR4/Cu reference, middle: Relative humidity sensitive coated resonator (psyllium), bottom: resonator with encapsulating and sensitive layers (beeswax and konjac).

Beeswax, from Sigma Aldrich, was weighted and melted at 80 °C in an adhesive well surrounding the resonator ($T_g$ = 62–67 °C). 3, 5 and 15 mg of wax was used to obtain a thickness of 50, 100 and 300 µm respectively. The wax was then cooled down on a flat surface to ambient temperature.

Following passivation, the humidity-sensitive coating will enable the response of the resonator to the ambient humidity and important characteristics to consider are its pattern definition, its adhesion, its sensitivity, reversibility, and hysteresis when exposed to variations in relative humidity.

We selected promising humidity-sensitive biodegradable materials (alginate, amylopectin, egg-albumin, PLGA, psyllium and konjac) and evaluated their behavior in the S-band for the first time.

Sodium alginate from brown algae is a biodegradable material with good hydrophilic behavior for humidity sensing [53]. Alginic acid sodium salt from Sigma Aldrich was dissolved in deionized water (DIW) in a 5 wt% and cast onto the resonator. Amylopectin, a polysaccharide sensitive to humidity [54], is one of the main components of starch. A 5 wt% DIW of amylopectin from maize from Sigma Aldrich was drop cast in the well, 25 µL using a pipette, and dried overnight. Egg-albumin, a class of water-soluble protein found in egg white, is composed of crosslinked amino acids with hydrophilic molecular bonds and exhibits excellent sensitivity to moisture [55]. Albumin from chicken egg white at 62–88% purity was ordered from Sigma Aldrich and mixed with DIW in 5 wt%. The solution was pipetted into a well and left to dry at 4 °C in the fridge to prevent layer cracking. As humidity sensitive layer, PLGA (85%PLA/15%PGA) was considered as it is water-soluble [56]. PLGA was prepared using PURASORB PLG 8531 pellets from Corbion and dissolved in 1,4dioxane (5 wt%) over 12 h and cast on the structure. Blond psyllium and konjac glucomannan are high-molecular weight polysaccharides abundant in nature with excellent film-forming abilities and extremely high water-absorption capabilities [57]. In the presence of water, psyllium and konjac take up to 50 and 100 times their weight in water producing a protein-rich mucilage [58]. Thanks to this hygroscopic nature, they have been used as swelling colorimetric sensors for humidity detection [57]. However, these interesting materials were never studied at ultra-high frequency or as coatings for humidity sensors. Konjac and psyllium seeds were obtained from a local pharmacy. They were mixed at 5 wt% in DIW. After water intake, the solutions were sonicated at 10000 rpm over 1 h to enable mucilage extraction. 50 µL from the mucilage solution was pipetted into the well and dried at room temperature.

Spiral copper resonators are coated with the various encapsulating and sensing materials. To confine the coated material into a homogenous active area, a rim of removable adhesive is used. The thickness of the humidity-sensitive layer was targeted to be 10 µm for all coatings investigated.

Finally, microstrip line resonator with encapsulation and humidity-sensitive layers stacked on each other were tested. A representation of the various types of tested devices (e.g: pristine microstrip line resonator used as reference, resonator coated with humidity sensitive layer, and the encapsulated resonator with the sensitive layer on top) is given in Fig. 1C.

### 2.2. Test setup and humidity profiles

The materials on the microstrip resonator were characterized using an in-house gas mixing system allowing the variation of the relative humidity in a test chamber [13]. The system consists of a pressurized dry air bottle and a bubbler linked to a climatic chamber where the microstrip resonator is placed. Valves allowed for the rapid switching and control of various relative humidity levels from 0% to 90%. The temperature and relative humidity have been monitored in real-time using an SHT30 sensor (Sensirion AG, Switzerland). A calibrated virtual network analyzer (E5071C Agilent) was used to measure the S12 signal (represents the power transferred from Port 1 to Port 2) of the microstrip line inside the chamber for frequencies between 2.5 GHz and 3.5 GHz.

Two humidity profiles were considered. First, a test to determine the sensor response and hysteresis was performed from 20% to 80% back down to 20% RH with 1 h steps and increments of 20% RH for a total of 7 h. Each measurement has been repeated 3 times with different samples for each configuration. A second test was conducted from 0% to 85%, cycled five times to evaluate the sensor recovery. A representation of the humidity profiles and elements of the testing setup is available in supplementary **Fig. S1**.

### 2.3. Simulation

To evaluate the influence of the addition of functional materials, encapsulant and sensing layer, over the active area of the microstrip structure, electromagnetic FEM simulations were performed using ANSYS HFSS. Standard FR4 parameters were set in the model using a dielectric constant of $\varepsilon = 4$ and a loss tangent of 0.02. The conductivity of bulk copper $\mu = 5.8e7$ S/m was used to model the transducing layer.

The model was evaluated from 2.5 GHz to 4 GHz. The simulation investigated the influence of the thickness of the encapsulation layer in dependence on its placement relative to the resonator allowing to conclude on an optimal coverage area for the sensing layer. The parameters of interest were the resulting frequency of resonance of the coated structure and its transmission signal S12.

## 3. Results and discussion

### 3.1. Preliminary materials screening and simulations

To define the influence of the area of the coating materials on the resonator characteristics, two simulations were performed. Firstly, simulation was applied to understand the effect of an increase of coating thickness on the frequency response of the resonator. Secondly, different coating dimensions were simulated to identify the minimal area at which we start seeing an influence over the frequency of resonance of the resonating spiral.

Fig. 2A shows the S12 recorded and the simulated response of the resonator coated with beeswax. The data was recorded at ambient temperature. Measurements at 0% and 80% RH on pristine FR4/Cu designs were used to model and fit the recorded values. The parameters for the simulated copper strip line on FR4 were tuned to fit with the recorded resonance value of 3.26 GHz. Similarly, using the recorded values for two different thicknesses of wax, 100 µm and 300 µm, the simulation was matched at 0% RH to reduce the simulation time. The frequency response was then simulated for various thicknesses as seen in shades of green in Fig. 2A. For the 300 µm thick wax coating, the recorded and simulated resonance frequencies perfectly matched at 3 GHz, while it slightly changed for a wax thickness of 100 µm, at 3.14 GHz, with a disparity of 15 MHz. As the coating thickness increases, the resonance frequency decreases. This can be explained by an increase in the capacitance surrounding the spiral resonator [45]. Higher radio-frequency losses are also introduced across a thicker wax layer which is represented by the reduction in the S12 signal in dB as the coating thickness is increased. In the frame of wireless applications, minimizing losses is important to enable long-range communication.

By tuning the simulation parameters to match the recorded samples, a permittivity for the beeswax coating of $\varepsilon = 3$ was extracted, corresponding to those reported in the literature [59]. This extracted permittivity was used to model the effect of the coverage area on the spiral resonator characteristics. In Fig. 2B, we can see a 3D representation of the simulated RF structure with the coating on top. Dimensions in the transversal direction lower than 5 mm lead to a shift in the resonance as the coating no longer fully covers the resonator spiral of size 4.4 × 5.4 $mm^2$. All coating dimensions bigger than 5 × 6 $mm^2$ did not have a significant impact on the resonance frequency. To ensure a reproducible and uniform coverage, a coated area of 6 × 8 $mm^2$ was considered to bypass any risk of misalignment of the adhesive well when depositing the various materials.

A preliminary selection of sensitive materials was conducted by evaluating the shift in resonant frequency for a relative humidity change of 20 to 80%. The thicknesses for the passivation and sensitive materials were established at 100 µm and 10 µm, respectively.

Beeswax has been identified as a good barrier to humidity (Fig. 3). A cover layer of 100 µm thick beeswax minimizes the susceptibility of the assessed signal to changes in relative humidity, even outperforming the pristine FR4 reference. The small change in resonance of the copper reference structure can be due to oxidation of the metal as no solder mask was applied when designing the circuit board. In comparison to beeswax, both bioresorbable polymers (POMaC and PGS) exhibit poor passivation properties despite extensive curing times.

For humidity sensing, among all materials tested, psyllium, egg-albumin and konjac were identified with the potential to provide a shift in resonance frequency exceeding 100 MHz for 60% change in relative humidity. The large frequency shift is obtained due to their rich hydrophilic protein concentrations [55]. Amylopectin and alginate induced a comparable shift of 29.35 and 44 MHz, respectively. PLGA displayed a very small response and acted more as an encapsulation than a sensitive coating, even outperforming POMaC and PGS. The methyl groups in the PLA portion slow down degradation but confer to it higher hydrophobic properties than PGA [56].

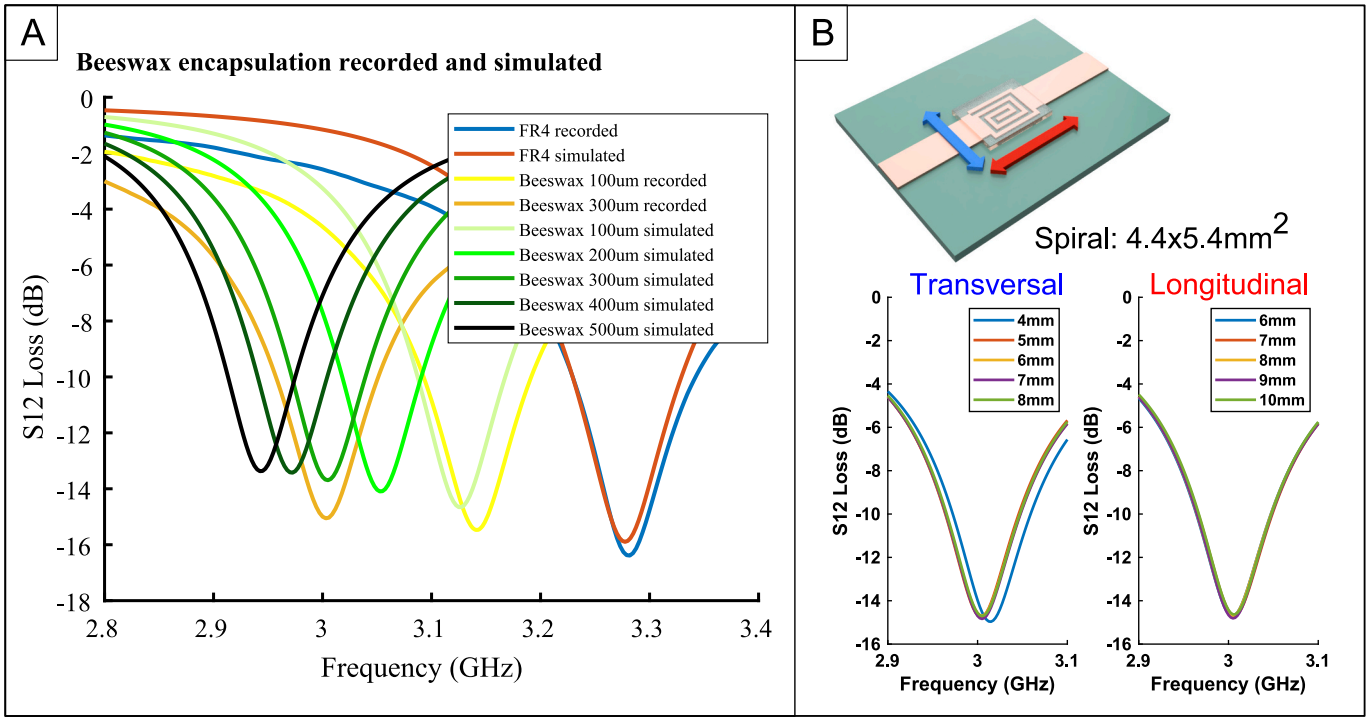


**Fig. 2.** A) Recorded and simulated effect of beeswax on resonator at 0% RH. B) 3D rendering and resonance dependency on coating dimensions along the longitudinal and transversal direction.

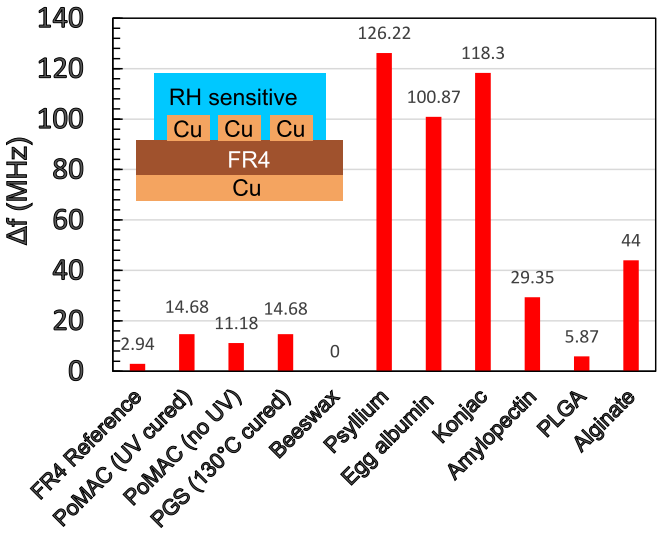


**Fig. 3.** Initial material screening, shift in resonance frequency from 20% to 80% RH.

Further studies were performed using only beeswax as encapsulant film and psyllium, egg-albumin and konjac as sensing layers (Fig. 1C) with results to be presented in the next section.

### 3.2. Biodegradable materials humidity response

#### 3.2.1. Response and hysteresis

Sensing layers of konjac have been tested with a thickness of 10 μm and 20 μm. The resonance frequency shifts from 3.23 GHz at 20% RH to 3.12 GHz at 80% RH for a 10 μm coating (Fig. 4A**).** As the humidity increases, the sharpness of the resonance is reduced due to an increase in the loss across the microstrip line. A coating thickness of 20 μm leads to a non-distinguishable resonance frequency at 80% RH due to RF losses (Fig. 4B**).** Finally, the thickness of all humidity-sensitive layers (konjac, psyllium and egg-albumin) was fixed at 10 μm to prevent this loss in the resonance behavior.

The resonance frequency and response of the resonator for the three selected humidity-sensitive materials were compared from 20% RH to 80% RH with increments of 20% RH (Fig. 4C**).** The changes in resonance frequency for psyllium, konjac and egg-albumin were $\Delta f_{psy} = -109 \pm 12$ *MHz*, $\Delta f_{kon} = -108 \pm 28$ *MHz* and $\Delta f_{EA} = -97 \pm 34$ *MHz*, respectively. The response does not follow a linear trend. This behavior can be explained by the non-linear mechanics of water sorption and swelling [60] at high relative humidity. For all three materials, the shift was in the similar range of 100 MHz, with psyllium displaying the best standard deviation across the samples.

Hysteresis was minimal in all 10 μm coated samples with the highest value of 15 MHz found for psyllium at 40% RH and 5 MHz and 4 MHz for konjac and egg-albumin, respectively, at 60% RH (Fig. 4C**).**

The variability of the response from 20% to 80% RH across samples is presented in supplementary **Fig. S3**. The variability in resonance frequency near 3GHz for the egg-albumin device was the worse, with a variation between samples of 146 MHz at 80% RH ($n = 3$), followed by psyllium with a variation of 123 MHz (n = 3) and finally konjac was the most reproducible with a variation of 45 MHz (n = 3). These variations are due to some irreproducibility in the fabrication process. The S12 data for each tested sample is reported in supplementary **Fig. S4.**

#### 3.2.2. Reversibility

Fig. 5A represents the S12 signal at 0% and 85% RH for konjac, psyllium and egg-albumin after 5 cycles. We can see that at 0% RH, they all have excellent reversibility. Contrasting with previous results, when the humidity is increased to 85%, psyllium's resonance remained stable moving by only 1 MHz after 5 cycles, while presenting a small change (7 MHz) for konjac and moving by 34 MHz for egg-albumin. The more reversible response for psyllium and konjac was obtained due to their super absorbent properties at high humidity [57]. Konjac is mainly amorphous [61] with D-mannose and D-glucose connected in random order across the acetyl groups giving the ability to reorganize the polymer chains in response to water absorption [62]. Similarly, Psyllium exhibits an unusual linkage of xylose and arabinose resulting in a highly branched arabinoxylan network [63,64] which allows water to be trapped within the network voids upon wetting and to be released upon de-wetting [65]. Fig. 5B represents the normalized frequency response computed as $NR = -\frac{f-f_0}{f_0-f_{85}}$ where $f$ is the resonant frequency and $f_0$ and $f_{85}$ are the resonant frequencies when saturation is reached at 0% RH and 85% RH. A Sensirion SHT35 sensor with a response time of 10 s and relative humidity accuracy of ±1.5% is used to record the dynamic of relative humidity in the chamber. Considering a response time at 63% of the saturation, the chamber's response and recovery times from 0% to 85% RH and from 85% to 0% RH are 60 s and 20 s. Similarly, for konjac, egg-albumin and psyllium where the frequency was recorded every 5

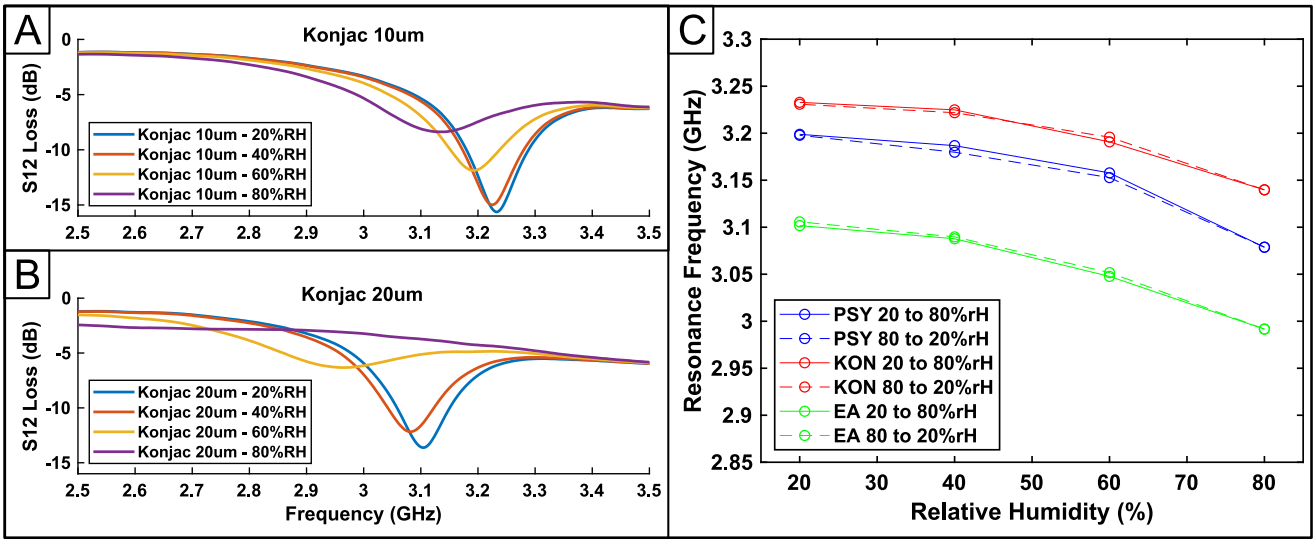


**Fig. 4.** Recorded S12 signal across 20% RH to 80% for (A) 10 μm and (B) 20 μm thick konjac. C) Humidity response and hysteresis for 10 μm of psyllium, konjac and egg-albumin represented by the resonance frequency shift as a function of the relative humidity.

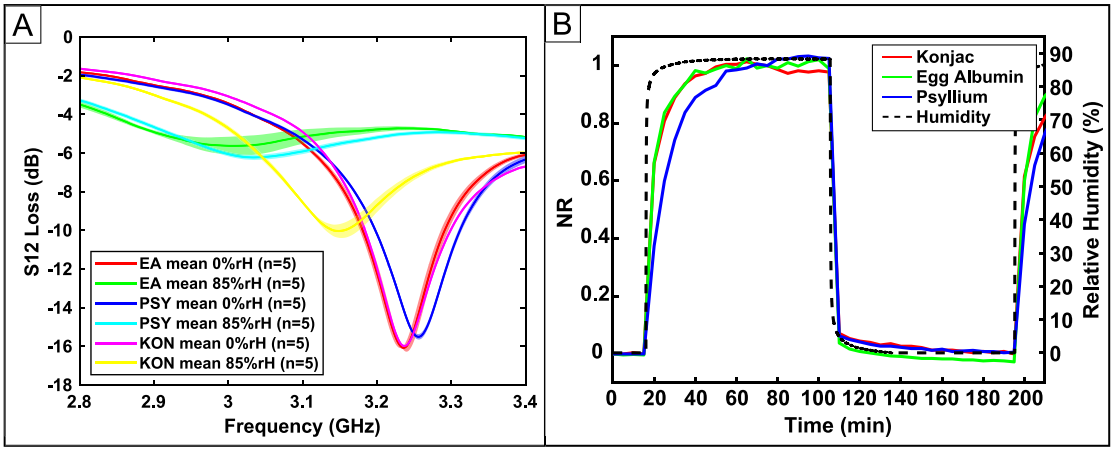


**Fig. 5.** A) Averaged S12 signal of the sensitive coatings, egg-albumin (EA), psyllium (PSY) and konjac (KON), at 0% and 85% RH, shaded area represents the standard deviation envelope of 5 cycles. B) Normalized resonant frequency response, $NR = -(f\text{-}f_0)/(f_0\text{-}f_{85})$ as a function of time for konjac, egg-albumin and psyllium compared to the humidity dynamic of the chamber measured with a humidity sensor from Sensirion.

min, we get a response time of <10 min for konjac and egg-albumin and <15 min for psyllium. For all three materials, the recovery is measured to be <5 min. Those response and recovery times were measurement for large and fast variations of humidity, going from a completely dry environment to a highly humid atmosphere. Therefore, for a large majority of the applicative environments for such sensors, the measured response and recovery times are expected to be smaller than those aforementioned.

### 3.2.3. *Stacked configuration response*

The final experiment consisted of analyzing the frequency response of the humidity-sensitive materials over the encapsulated resonator. Similarly to previous samples preparation, konjac, psyllium and egg-albumin were drop casted onto a well over the beeswax-coated resonator. Egg-albumin coating failed to remain on the wax and underwent delamination despite treating the wax with oxygen plasma and/or APTES treatment. The peeling of egg-albumin over the wax can be explained by the incompatibility between the hydrophobic character of the wax and the hydrophilic nature of the protein in DIW during fabrication. The psyllium and konjac layers were able to adhere due to the sticky nature of the mucilage solution. Nevertheless, oxygen plasma was used before their drop-casting to ensure proper adhesion.

To prevent too many losses and ensure proper passivation, beeswax coatings with a thickness of 50 to 100 µm were implemented, onto which, 10 $\mu$m of konjac and psyllium were deposited. The response of the stacked-microstrip line was measured from 20% and 80% RH. Fig. 6A depicts the transmission signal of psyllium-coated wax. As the thickness of wax increases, the initial resonance at 20% RH is reduced. When the wax is present, the response to an increase in humidity is reduced. This is expected as the sensitive layer is now further away from the resonating structure. The shift in frequency from 20% to 80% for 10 µm/50 µm and 10 µm/100 µm psyllium/wax resonators was measured to be very close at 23 MHz and 22 MHz, respectively. Compared to a resonator not coated with wax, this represents a reduction in sensitivity by a factor of 4.7 and 4.9, respectively. In this case, the encapsulation acted dominantly on the S12 signal. Alike, Fig. 6B shows the response for konjac/beeswax devices. The dominating effect of the wax was less pronounced, with a frequency shift for a 60% RH variation of 56 MHz and 88 MHz for 10 µm/50 µm and 10 µm/100 µm konjac/wax combinations, respectively. This different response behavior between konjac and psyllium needs to be further investigated. One assumption could be the difference in swelling between both sensing materials at high humidity levels. The sensitivity was also higher for konjac and only reduced by a factor of 2 and 1.25 for a wax thickness of 50 µm and 100 µm, respectively. The hysteresis data for both configurations are available in supplementary **Fig. S5**. A hysteresis of only 3 MHz and 4 MHz was measured for psyllium and konjac, respectively. The sensor response becomes non-linear at higher levels of humidity (>60% RH) due to changes in the humidity adsorption behavior within the biopolymers as already notified in the literature [11,66].

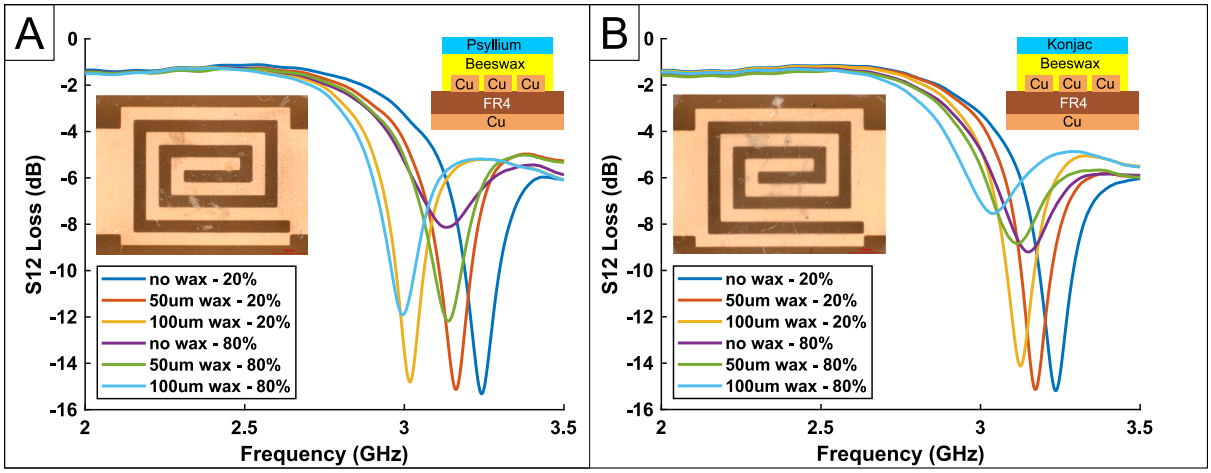


**Fig. 6.** A) S12 signal for 50 µm and 100 µm beeswax stacked with 10 um psyllium. B) S12 signal for 50 and 100 um beeswax stacked with 10 µm konjac.

In the end, both psyllium and konjac over beeswax displayed promising responses to relative humidity at high frequency and low hysteresis with konjac being more sensitive.

## 4. Conclusions

Using a copper/FR4 microstrip line resonating at 3.3 GHz, we studied the humidity interaction in the S-band frequency band of various biodegradable materials from 20% to 80% relative humidity. For the first time biodegradable moisture sensitive layers were analyzed over a resonator operating at ultra-high frequency and then combined with a passivation. With the support of electromagnetic simulations, the optimal area to cover the resonator was defined for the encapsulant and humidity-sensitive materials. As encapsulation, beeswax was identified to provide excellent protection against moisture with a stable resonant frequency of the resonator over the whole humidity range tested. Egg-albumin and the super absorbent polymers, konjac and psyllium, provided the best responses to humidity with sensitivities higher than 1.75 MHz/RH% and the lowest hysteresis. Reversibility of the response over multiple humidity cycles was the best for psyllium and konjac with a maximum change of only 5 MHz. The response times for a 0% to 85% humidity change was of 15 min for psyllium, down to 10 min for konjac and egg-albumin and the recovery time from 85% to 0% RH of all three materials was <5 min. An original RF humidity-sensitive stack configuration is finally proposed with those super absorbent polymers being coated over a beeswax encapsulant layer. The combination involving 10 μm konjac and 100 μm beeswax showed the highest sensitivity of 1.46 MHz/RH% with only 4 MHz hysteresis in the resonance across the full humidity range.

We demonstrate that performing eco-friendly humidity-sensitive materials can be implemented over an encapsulated S-band resonator for humidity monitoring. The next step is to implement this stacked configuration in a fully biodegradable microstrip line made on paper. This biodegradable humidity sensitive layer / encapsulant stack can pave the way for fully biodegradable paper-based wireless sensors.

## Declaration of Competing Interest

The authors declare that they have no known competing financial interests or personal relationships that could have appeared to influence the work reported in this paper.

## Data availability

Data will be made available on request.

## Acknowledgments

The authors kindly acknowledge funding from the Swiss National Science Foundation and Innosuisse BRIDGE Discovery program for the project “GREENsPACK—Green Smart Packaging” (Grant No.: 40B2-0_187223/1).

## Appendix A. Supplementary data

Supplementary data to this article can be found online at https://doi.org/10.1016/j.mne.2023.100185.

## References

[1] V. Forti, C.P. Baldé, R. Kuehr, G. Bel, The Global E-waste Monitor, Quantities, flows, and the circular economy potential. 2020. Bonn/Geneva/Rotterdam: United Nations University (UNU)/United Nations Institute for Training and Research (UNITAR) - co-hosted SCYCLE Programme, International Telecommunication Union (ITU) & International Solid Waste Association (ISWA) 2020, 2020.

[2] S.V. Akram, R. Singh, A. Gehlot, M. Rashid, A.S. AlGhamdi, S.S. Alshamrani, et al., Role of wireless aided Technologies in the Solid Waste Management: a comprehensive review, Sustainability 13 (2021) 13104, https://doi.org/10.3390/su132313104.

[3] S. Zhang, Y. Gu, A. Tang, B. Li, B. Li, D. Pan, et al., Forecast of future yield for printed circuit board resin waste generated from major household electrical and electronic equipment in China, J. Clean. Prod. 283 (2021), 124575, https://doi.org/10.1016/j.jclepro.2020.124575.

[4] Z. Lv, Practical application of internet of things in the creation of intelligent services and environments, Front. Internet Things 1 (2022), 912388, https://doi.org/10.3389/friot.2022.912388.

[5] C. Aliaga, B. Ferreira, M. Hortal, M.Á. Pancorbo, J.M. López, F.J. Navas, Influence of RFID tags on recyclability of plastic packaging, Waste Manag. 31 (2011) 1133–1138, https://doi.org/10.1016/j.wasman.2010.12.015.

[6] H. Tai, Z. Duan, Y. Wang, S. Wang, Y. Jiang, Paper-based sensors for gas, humidity, and strain detections: a review, ACS Appl. Mater. Interfaces 12 (2020) 31037–31053, https://doi.org/10.1021/acsami.0c06435.

[7] Z. Duan, Y. Jiang, M. Yan, S. Wang, Z. Yuan, Q. Zhao, et al., Facile, flexible, cost-saving, and environment-friendly paper-based humidity sensor for multifunctional applications, ACS Appl. Mater. Interfaces 11 (2019) 21840–21849, https://doi.org/10.1021/acsami.9b05709.

[8] C. Gaspar, J. Olkkonen, S. Passoja, M. Smolander, Paper as active layer in inkjet-printed capacitive humidity sensors, Sensors 17 (2017) 1464, https://doi.org/10.3390/s17071464.

[9] A. Beniwal, P. Ganguly, A.K. Aliyana, G. Khandelwal, R. Dahiya, Screen-printed graphene-carbon ink based disposable humidity sensor with wireless communication, Sensors Actuators B Chem. 374 (2023), 132731, https://doi.org/10.1016/j.snb.2022.132731.

[10] X. Zhang, D. He, Q. Yang, M.Z. Atashbar, Rapid, highly sensitive, and highly repeatable printed porous paper humidity sensor, Chem. Eng. J. 433 (2022), 133751, https://doi.org/10.1016/j.cej.2021.133751.

[11] X. Aeby, J. Bourely, A. Poulin, G. Siqueira, G. Nyström, D. Briand, Printed humidity sensors from renewable and biodegradable materials. Adv, Mater. Technol. (2022) 2201302, https://doi.org/10.1002/admt.202201302.

[12] Z. Duan, Q. Zhao, S. Wang, Q. Huang, Z. Yuan, Y. Zhang, et al., Halloysite nanotubes: natural, environmental-friendly and low-cost nanomaterials for high-performance humidity sensor, Sensors Actuators B Chem. 317 (2020), 128204, https://doi.org/10.1016/j.snb.2020.128204.

[13] F. Molina-Lopez, D. Briand, N.F. de Rooij, All additive inkjet printed humidity sensors on plastic substrate, Sensors Actuators B Chem. 166–167 (2012) 212–222, https://doi.org/10.1016/j.snb.2012.02.042.

[14] A.V. Quintero, N. Frolet, D. Marki, A. Marette, G. Mattana, D. Briand, et al., Printing and encapsulation of electrical conductors on polylactic acid (PLA) for sensing applications, in: 2014 IEEE 27th Int. Conf. Micro Electro Mech. Syst. MEMS, San Francisco, CA, USA, IEEE, 2014, pp. 532–535, https://doi.org/10.1109/MEMSYS.2014.6765695.

[15] J. Zikulnig, S. Lengger, L. Rauter, L. Neumaier, S. Carrara, J. Kosel, Sustainable printed chitosan-based humidity sensor on flexible biocompatible polymer substrate, IEEE Sens. Lett. 6 (2022) 1–4, https://doi.org/10.1109/LSENS.2022.3224768.

[16] E. Wawrzynek, C. Baumbauer, A.C. Arias, Characterization and comparison of biodegradable printed capacitive humidity sensors, Sensors 21 (2021) 6557, https://doi.org/10.3390/s21196557.

[17] M.U. Khan, Q.M. Saqib, G. Hassan, J. Bae, All printed organic humidity sensor based on egg albumin, Sens. Bio-Sens Res. 28 (2020), 100337, https://doi.org/10.1016/j.sbsr.2020.100337.

[18] M. Sajid, S. Aziz, G.B. Kim, S.W. Kim, J. Jo, K.H. Choi, Bio-compatible organic humidity sensor transferred to arbitrary surfaces fabricated using single-cell-thick onion membrane as both the substrate and sensing layer, Sci. Rep. 6 (2016) 30065, https://doi.org/10.1038/srep30065.

[19] A. Falco, A. Marín-Sánchez, F.C. Loghin, E. Castillo, A. Salinas-Castillo, J. F. Salmerón, et al., Paper and salt: biodegradable NaCl-based humidity sensors for sustainable electronics, Front. Electron. 3 (2022), 838472, https://doi.org/10.3389/felec.2022.838472.

[20] Y. Zheng, L. Wang, L. Zhao, D. Wang, H. Xu, K. Wang, et al., A flexible humidity sensor based on natural biocompatible silk fibroin films, Adv. Mater. Technol. 6 (2021) 2001053, https://doi.org/10.1002/admt.202001053.

[21] X. Huang, T. Leng, T. Georgiou, J. Abraham, R. Raveendran Nair, K.S. Novoselov, et al., Graphene oxide dielectric permittivity at GHz and its applications for wireless humidity Sensing, Sci. Rep. 8 (2018) 43, https://doi.org/10.1038/s41598-017-16886-1.

[22] L. Khtaoui, M. Laghrouche, F. Fernane, A. Chaouchi, High-sensitivity humidity sensor based on natural hydroxyapatite, J. Mater. Sci. Mater. Electron. 32 (2021) 8668–8686, https://doi.org/10.1007/s10854-021-05538-w.

[23] F. Bibi, C. Guillaume, A. Vena, N. Gontard, B. Sorli, Wheat gluten, a bio-polymer layer to monitor relative humidity in food packaging: electric and dielectric characterization, Sensors Actuators A Phys. 247 (2016) 355–367, https://doi.org/10.1016/j.sna.2016.06.017.

[24] Z. Duan, Z. Yuan, Y. Jiang, Q. Zhao, Q. Huang, Y. Zhang, et al., Power generation humidity sensor based on primary battery structure, Chem. Eng. J. 446 (2022), 136910, https://doi.org/10.1016/j.cej.2022.136910.

[25] S. Conti, F. Nepa, S. Di Pascoli, I. Brunetti, L. Pimpolari, X. Song, et al., Hybrid flexible NFC sensor on paper, IEEE J. Flex. Electron. (2023) 1, https://doi.org/10.1109/JFLEX.2023.3238682.

[26] A.V. Quintero, F. Molina-Lopez, E.C.P. Smits, E. Danesh, J. van den Brand, K. Persaud, et al., Smart RFID label with a printed multisensor platform for environmental monitoring, Flex Print Electron. 1 (2016), 025003, https://doi.org/10.1088/2058-8585/1/2/025003.

[27] J. Han, N. Xu, J. Yu, Y. Wang, Y. Xiong, Y. Wei, et al., Energy autonomous paper modules and functional circuits, Energy Environ. Sci. 15 (2022) 5069–5081, https://doi.org/10.1039/D2EE02557D.
[28] Mc Gee, Collins Anandarajah, A review of Chipless remote Sensing solutions based on RFID technology, Sensors 19 (2019) 4829, https://doi.org/10.3390/s19224829.
[29] W. Yang, X. Cheng, Z. Guo, Q. Sun, J. Wang, C. Wang, Design, fabrication and applications of flexible RFID antennas based on printed electronic materials and technologies, J. Mater. Chem. C 11 (2023) 406–425, https://doi.org/10.1039/D2TC03736J.
[30] F. Requena, N. Barbot, D. Kaddour, Perret E. Chipless, RFID temperature and humidity sensing, in: 2021 IEEE MTT- Int. Microw. Symp. IMS, Atlanta, GA, USA, IEEE, 2021, pp. 545–548, https://doi.org/10.1109/IMS19712.2021.9574942.
[31] S. Preradovic, N.C. Karmakar, Multiresonator-Based Chipless RFID: Barcode of the Future, Springer, New York, 2012.
[32] A. Vorobyov, C. Bever, P. Nussbaum, D. Schmid, Chipless biodegradable tags, Theoretical Performance Estimation: Invited Paper, in: 2022 IEEE 2nd Ukr. Microw. Week UkrMW, IEEE, Ukraine, 2022, pp. 01–05, https://doi.org/10.1109/UkrMW58013.2022.10037075.
[33] J. Anum Satti, A. Habib, H. Anam, S. Zeb, Y. Amin, J. Loo, et al., Miniaturized humidity and temperature sensing RFID enabled tags, Int. J. RF Microw. Comput-Aided Eng. 28 (2018), e21151, https://doi.org/10.1002/mmce.21151.
[34] L. Liu, L. Chen, Characteristic analysis of a Chipless RFID sensor based on multi-parameter Sensing and an intelligent detection method, Sensors 22 (2022) 6027, https://doi.org/10.3390/s22166027.
[35] A. Zareei, S. Gopalakrishnan, Z. Mutlu, Z. He, S. Peana, H. Wang, et al., Highly conductive copper–silver bimodal paste for low-cost printed electronics, ACS Appl. Electron. Mater. 3 (2021) 3352–3364, https://doi.org/10.1021/acsaelm.1c00345.
[36] Y. Feng, L. Xie, Q. Chen, L.-R. Zheng, Low-cost printed Chipless RFID humidity sensor tag for intelligent packaging, IEEE Sensors J. 15 (2015) 3201–3208, https://doi.org/10.1109/JSEN.2014.2385154.
[37] M. Borgese, F.A. Dicandia, F. Costa, S. Genovesi, G. Manara, An inkjet printed Chipless RFID sensor for wireless humidity monitoring, IEEE Sensors J. 17 (2017) 4699–4707, https://doi.org/10.1109/JSEN.2017.2712190.
[38] S. Gopalakrishnan, S. Sedaghat, A. Krishnakumar, Z. He, H. Wang, R. Rahimi, Wireless humidity sensor for smart packaging via one-step laser-induced patterning and nanoparticle formation on metallized paper, Adv. Electron Mater. 8 (2022) 2101149, https://doi.org/10.1002/aelm.202101149.
[39] Emd Amin, MdS Bhuiyan, N.C. Karmakar, B. Winther-Jensen, Development of a low cost printable Chipless RFID humidity sensor, IEEE Sensors J. 14 (2014) 140–149, https://doi.org/10.1109/JSEN.2013.2278560.
[40] J. Yeo, J.-I. Lee, Y. Kwon, Humidity-Sensing Chipless RFID tag with enhanced sensitivity using an interdigital capacitor structure, Sensors 21 (2021) 6550, https://doi.org/10.3390/s21196550.
[41] P. Fathi, S. Bhattacharya, N.C. Karmakar, Dual-polarized keratin-based UWB Chipless RFID relative humidity sensor, IEEE Sensors J. 22 (2022) 1924–1932, https://doi.org/10.1109/JSEN.2021.3135500.
[42] A. Sudheshwar, N. Malinverno, R. Hischier, B. Nowack, C. Som, The need for design-for-recycling of paper-based printed electronics – a prospective comparison with printed circuit boards, Resour. Conserv. Recycl. 189 (2023), 106757, https://doi.org/10.1016/j.resconrec.2022.106757.
[43] S. Gopalakrishnan, J. Waimin, A. Zareei, S. Sedaghat, N. Raghunathan, A. Shakouri, et al., A biodegradable chipless sensor for wireless subsoil health monitoring, Sci. Rep. 12 (2022) 8011, https://doi.org/10.1038/s41598-022-12162-z.
[44] S. Preradovic, I. Balbin, N.C. Karmakar, G.F. Swiegers, Multiresonator-based Chipless RFID system for low-cost item tracking, IEEE Trans. Microw Theory Tech. 57 (2009) 1411–1419, https://doi.org/10.1109/TMTT.2009.2017323.
[45] Y.K. Awasthi, H. Singh, M. Sharma, S. Kumari, A.K. Verma, Computer-aided design-based circuit model of microstrip line for terahertz interconnects technology, J. Eng. Des. 2017 (2017) 512–526, https://doi.org/10.1049/joe.2017.0078.
[46] M. Sadiku, S. Musa, S. Nelatury, Comparison of approximate formulas for the capacitance of microstrip line, in: Proc. 2007 IEEE SoutheastCon, Richmond, VA, USA, IEEE, 2007, pp. 427–432, https://doi.org/10.1109/SECON.2007.342939.
[47] L. Corchia, G. Monti, E.D. Benedetto, L. Tarricone, A Chipless humidity sensor for wearable applications, in: 2019 IEEE Int. Conf. RFID Technol. Appl. RFID-TA, IEEE, Pisa, Italy, 2019, pp. 174–177, https://doi.org/10.1109/RFID-TA.2019.8892048.
[48] A. Sohrabi, P. Mojir Shaibani, M.H. Zarifi, M. Daneshmand, T. Thundat, A novel technique for rapid vapor detection using swelling polymer covered microstrip ring resonator, in: 2014 IEEE MTT- Int. Microw. Symp. IMS2014, IEEE, Tampa, FL, USA, 2014, pp. 1–4, https://doi.org/10.1109/MWSYM.2014.6848306.
[49] J.-S. Shim, J.A. Rogers, S.-K. Kang, Physically transient electronic materials and devices, Mater. Sci. Eng. R. Rep. 145 (2021), 100624, https://doi.org/10.1016/j.mser.2021.100624.
[50] C.M. Boutry, Y. Kaizawa, B.C. Schroeder, A. Chortos, A. Legrand, Z. Wang, et al., A stretchable and biodegradable strain and pressure sensor for orthopaedic application, Nat. Electron. 1 (2018) 314–321, https://doi.org/10.1038/s41928-018-0071-7.
[51] R.T. Tran, P. Thevenot, D. Gyawali, J.-C. Chiao, L. Tang, J. Yang, Synthesis and characterization of a biodegradable elastomer featuring a dual crosslinking mechanism, Soft Matter 6 (2010) 2449, https://doi.org/10.1039/c001605e.
[52] R. Rai, M. Tallawi, A. Grigore, A.R. Boccaccini, Synthesis, properties and biomedical applications of poly(glycerol sebacate) (PGS): a review, Prog. Polym. Sci. 37 (2012) 1051–1078, https://doi.org/10.1016/j.progpolymsci.2012.02.001.
[53] Y.C. Han, X.Y. Kong, W. Wu, J.S. Li, X. Yang, Y.J. Guo, et al., Environment-friendly surface acoustic wave humidity sensor with sodium alginate sensing layer, Micro. Nano. Eng. 15 (2022), 100127, https://doi.org/10.1016/j.mne.2022.100127.
[54] J.J.G. van Soest, P. Essers, Influence of amylose-amylopectin ratio on properties of extruded starch plastic sheets, J. Macromol. Sci. Part A 34 (1997) 1665–1689, https://doi.org/10.1080/10601329708010034.
[55] H.M. Mutee Ur Rehman, M.M. Rehman, M. Saqib, S. Ali Khan, M. Khan, Y. Yang, et al., Highly efficient and wide range humidity response of biocompatible egg white thin film, Nanomaterials 11 (2021) 1815, https://doi.org/10.3390/nano11071815.
[56] H.K. Makadia, S.J. Siegel, Poly lactic-co-glycolic acid (PLGA) as biodegradable controlled drug delivery carrier, Polymers 3 (2011) 1377–1397, https://doi.org/10.3390/polym3031377.
[57] M. Momtaz, J. Chen, High-performance colorimetric humidity sensors based on Konjac Glucomannan, ACS Appl. Mater. Interfaces 12 (2020) 54104–54116, https://doi.org/10.1021/acsami.0c16495.
[58] F. Ma, R. Wang, X. Li, W. Kang, A.E. Bell, D. Zhao, et al., Physical properties of mucilage polysaccharides from Dioscorea opposita Thunb, Food Chem. 311 (2020), 126039, https://doi.org/10.1016/j.foodchem.2019.126039.
[59] S.P. Chakyar, T.A. Shanto, A. Murali, S.K. Sikha, N. Paul, J. Andrews, et al., Measurement of dielectric constant of waxes at different temperatures using split ring resonator structure, in: 2016 IEEE MTT- Int. Microw. RF Conf. IMaRC, IEEE, New Delhi, 2016, pp. 1–4, https://doi.org/10.1109/IMaRC.2016.7939638.
[60] C.K. Pandiyarajan, O. Prucker, J. Rühe, Humidity driven swelling of the surface-attached poly(*N* -alkylacrylamide) hydrogels, Macromolecules 49 (2016) 8254–8264, https://doi.org/10.1021/acs.macromol.6b01379.
[61] J. Li, T. Ye, X. Wu, J. Chen, S. Wang, L. Lin, et al., Preparation and characterization of heterogeneous deacetylated konjac glucomannan, Food Hydrocoll. 40 (2014) 9–15, https://doi.org/10.1016/j.foodhyd.2014.02.001.
[62] K. Katsuraya, K. Okuyama, K. Hatanaka, R. Oshima, T. Sato, K. Matsuzaki, Constitution of konjac glucomannan: chemical analysis and 13C NMR spectroscopy, Carbohydr. Polym. 53 (2003) 183–189, https://doi.org/10.1016/S0144-8617(03)00039-0.
[63] L. Yu, G.E. Yakubov, W. Zeng, X. Xing, J. Stenson, V. Bulone, et al., Multi-layer mucilage of Plantago ovata seeds: rheological differences arise from variations in arabinoxylan side chains, Carbohydr. Polym. 165 (2017) 132–141, https://doi.org/10.1016/j.carbpol.2017.02.038.
[64] A. Tóth, K. Halász, Characterization of edible biocomposite films directly prepared from psyllium seed husk and husk flour, Food Packag. Shelf Life 20 (2019), 100299, https://doi.org/10.1016/j.fpsl.2019.01.003.
[65] J.-K. An, W.-B. Wang, A.-Q. Wang, Preparation and swelling properties of a pH-sensitive superabsorbent hydrogel based on psyllium gum, Starch - Stärke 62 (2010) 501–507, https://doi.org/10.1002/star.200900244.
[66] T. Fei, H. Zhao, K. Jiang, X. Zhou, T. Zhang, Polymeric humidity sensors with nonlinear response: properties and mechanism investigation, J. Appl. Polym. Sci. 130 (2013) 2056–2061, https://doi.org/10.1002/app.39400.